Chapter 7
Symmetry and Non-empirical Calculations of Structure and Properties of Single- and Double-Wall $SrTiO_3$ Nanotubes

R.A. Evarestov and A.V. Bandura

Abstract A large-scale first-principles simulation of the structure and stability of $SrTiO_3$ single- and double-wall nanotubes with different chiralities has been performed for the first time using the periodic PBE0 LCAO method. The initial structures of nanotubes have been obtained by rolling up slabs consisting of two and four alternating (001) SrO and TiO_2 planes. In the majority of the considered cases the inner or outer TiO_2 shells of 4-layer nanotubes undergo a considerable reconstruction due to shrinkage or stretching of interatomic distances. Double-wall nanotubes constructed from 2-layer single-wall nanotubes with the intertube distance less than 4.5–5.0 Å merge to stable polyhedron-shaped tubular objects consisting of blocks with a distorted cubic perovskite structure.

Keywords Perovskites • Nanotubes • PBE0 LCAO method

7.1 Introduction

Nanostructures of complex metal oxides with perovskite structure $ATiO_3$ (A = Ca, Sr, Ba, Pb) have a potential application as nanosized ferroelectrics and memory elements and have recently attracted significant interest because of their unique physical properties [1, 2]. Among these, strontium titanate (STO) serves as one of the most versatile functional materials in a wide range of technological uses. Several studies have been focused on investigation of producing nanotubes (NTs) composed of $SrTiO_3$ and, moreover, on arranging them into highly organized arrays that most closely resemble single-crystal properties while composing a large-scale tubular architecture [3].

R.A. Evarestov (✉) • A.V. Bandura
Department of Quantum Chemistry, St. Petersburg State University, Universitetskii pr. 26, Peterhof, 198504 St. Petersburg, Russia
e-mail: re1973@re1973.spb.edu

Y.N. Shunin and A.E. Kiv (eds.), *Nanodevices and Nanomaterials for Ecological Security*, NATO Science for Peace and Security Series B: Physics and Biophysics, DOI 10.1007/978-94-007-4119-5_7,
© Springer Science+Business Media Dordrecht 2012

First-principles Density Functional Theory (DFT)-based calculations have complemented the experimental developments both on the bulk cubic titanates and on STO NTs. To the best of our knowledge, first principles DFT calculations for perovskite NTs are absent. The preliminary results of our calculations on single-wall STO NTs are reported in Ref. [4]. In the present paper we give the results of the first double-wall STO nanotubes DFT-based calculations in comparison with those obtained for single-wall nanotubes.

7.2 Symmetry of $SrTiO_3$ Nanotubes and the Computational Approach

The symmetry and structure of single-wall (SW) nanotubes can be simply described using the so-called layer folding, which means the construction of the cylindrical surfaces of NT by rolling up the two-periodic (2D) crystalline layers (sheets and slabs) [5]. The nanotube is defined by a translation vector $\mathbf{L} = l_1\mathbf{a} + l_2\mathbf{b}$ and a chiral vector $\mathbf{R} = n_1\mathbf{a} + n_2\mathbf{b}$, ($l_1$, l_2, n_1 and n_2 are integers, **a** and **b** – are translation vectors of the plane lattice). The nanotube of the chirality (n_1, n_2) is obtained by folding the layer in a way that the chiral vector **R** becomes a circumference of NT. The greatest common divisor N of n_1 and n_2, $N = G(n_1, n_2)$, defines the order of the NT pure rotation axis.

In the case of STO, the folding procedure is applied to the most stable (001) slab cut from the bulk crystal with a cubic space group 221 ($Pm\overline{3}m$). The initial slab symmetry is described as a square plane lattice. The slab layer symmetry group depends on the number of layers included in the folding procedure. Figure 7.1 shows 2 and 4-layer slabs cut from the bulk STO with one formula unit in the bulk unit cell. For the even number of layers there is a slab layer group P4*mm* (55). As it follows from the results of Ref. [5], after the rolling procedure this layer group generates single-wall (n, 0) and (n, n) NTs with the line symmetry groups belonging to family 11 (point symmetry D_{nh}) and to family 13 (point symmetry D_{2nh}), respectively.

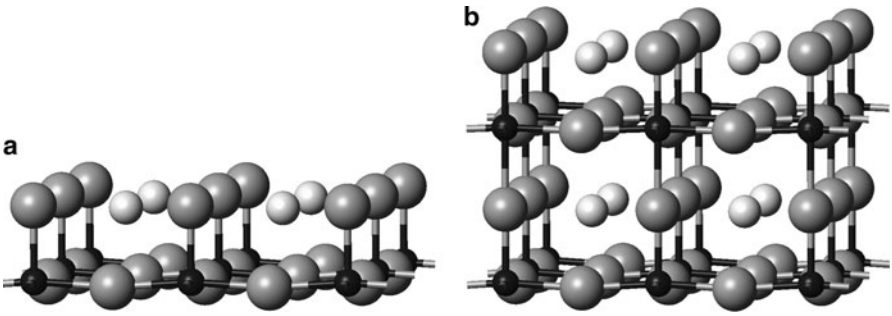

Fig. 7.1 $SrTiO_3$ slabs consisting of two (**a**) and four (**b**) alternating (001) SrO and TiO_2 atomic planes which have been used for nanotubes construction (*side view*). Legend: O – *grey balls*, Ti – *small dark balls*, Sr – *small light balls*

The line symmetry group of a double-wall (DW) nanotube can be found as the intersection of the symmetry groups of its single-wall constituents [6]. Let (n_1, n_2) and (n_1', n_2') define the chiral vectors of single-wall constituents of DWNT. The DWNT axial point group C_N is the principal axis subgroup of DWNT line group with $N = G(n, n') = G(n_1, n_2, n_1', n_2')$. Only NTs composed exclusively of either (n, n) or $(n, 0)$ SW constituents may have additional mirror and glide planes, as well as a rotoreflectional axis.

The STO DWNTs $(n_1, 0)@(n_2, 0)$ and $(n_1, n_1)@(n_2, n_2)$ are commensurate; the minimal translation period for such DWNTs is the same as for constituents. The symmetry group of DWNT $(n_1, 0)@(n_2, 0)$ belongs to the same family 11 as its SW constituents. It has been shown [6, 7] that two possibilities arise for DWNTs $(n_1, n_1)@(n_2, n_2)$: (*i*) both n_1/N and n_2/N are odd; (*ii*) one or both n_1/N and n_2/N are even. In the case (*i*), the line symmetry groups are the same as for their SW constituents and belong to family 13 (the order of screw axis is 2 N). In the case (*ii*), the rotations around the screw axis of order 2 N are changed by rotations around the pure rotation axis of order N so that DWNT line symmetry groups belong to family 11.

All our calculations have been carried out using the periodic PBE0 LCAO method via CRYSTAL-2009 computer code [8]. CRENBL small-core pseudopotentials [9] and the corresponding basis sets have been used for Sr and Ti atoms. The diffuse exponents less than 0.1 a.u. were removed and exponents of other polarization functions have been reoptimized for the periodic calculations. All-electron basis set for O atom has been taken from Ref. [10]. The chosen method provides a good quality of the calculated STO bulk properties. Thus, the optimized lattice constant of cubic STO (3.89 Å) is very close to the experimental value (3.90 Å).

The initial structures of SWNTs have been obtained by rolling up STO slabs consisting of two or four alternating (001) SrO and TiO_2 atomic planes (Fig. 7.1). The structure of slabs has been optimized before folding. The optimized lattice constants of two-dimensional square lattices are slightly decreased (by about 0.05 Å) compared to the bulk value. The atomic positions on the boundary planes exhibit noticeable relaxation which, in general, resembles that on the surface of the thicker STO slabs [11, 12]. Upon the relaxation, each atomic plane is split into two or three planes that still remain to be relatively close to each other, thus, forming a separate layer. The optimized slab thickness (the difference in z-coordinate of top and bottom oxygens) is 1.99 Å for a two-layer slab and 5.90 for a four-layer slab.

Positions of all atoms have been optimized to obtain the most stable NT structure, preserving the rototranslational symmetry only. Other symmetry constraints on NTs (second-order U axes normal to the tube axis, and reflection planes) were removed during atomic relaxation. One-dimensional Brillouin zone has been sampled with 16 (for chiralities $(n, 0)$) or 12 (for chiralities (n, n)) k-points.

The stability of SWNTs relative to the relaxed slab is described by the strain energy, $E_{\mathrm{str}} = E_l(\mathrm{NT})/l - E_m(\mathrm{slab})/m$, where $E_l(\mathrm{NT})$ – is the total energy of the NT unit cell consisting of l bulk formula units, and $E_m(\mathrm{slab})$ – is the total energy of the slab unit cell including m bulk formula units. To study the stability of DWNTs we use two quantities: (1) binding energy, E_{bind} – the energy gain upon combining of

two constituent SWNTs, and (2) reformative energy, E_{ref} – the difference between the energy of (relaxed or reformed) DWNT and the energy of SWNT with the same number of atoms. Both quantities are reduced per one STO formula unit.

7.3 Single-Wall Nanotubes

We consider stoichiometric SWNT of two thicknesses, which were rolled up from STO slabs initially consisting of two or four alternating (001) SrO and TiO_2 atomic planes (Fig. 7.1). Two different NTs can be constructed for each chirality: (I) with SrO outer shell, and (II) with TiO_2 outer shell. The inner shell has an alternate composition for the adopted even number of planes in the slab. The tube thickness w has been calculated as a half of the difference between the external and internal diameters. External and internal diameters of NT are estimated as a double distance from the NT axis to the most remote or the nearest atom, correspondingly. Almost in all considered NTs the most remote and the nearest atoms – are oxygens. While the walls of 2-layer NTs are rather thin ($w \approx 2$ Å), the walls of 4-layer NTs are three times thicker ($w \approx 6$ Å). The obtained results are given in Tables 7.1 and 7.2. The chiralities chosen for computations are intended to be representative and most of them are used for the analysis of DWNT properties (see Sect. 7.4).

After slab folding, the inner and outer atomic shells undergo a considerable stress due to stretching or shrinking of the interatomic distances relative to those in the initial relaxed slab. The less is the tube diameter and the thicker is the tube wall, the greater is the strain. The most critical is the repulsion between the nearest oxygen atoms in the inner shells and, as a rule, the distance between them must not be less than 2.7–2.6 Å. The inner and outer shells are strained in the opposite directions, thus, reducing the tension in the former may increase the tension in the latter.

Table 7.1 Properties[a] of $SrTiO_3$ two-layer single-wall nanotubes

	Type I (SrO outer shell)				Type II (TiO_2 outer shell)			
Chirality	L (Å)	d (Å)	E_{str} (kJ/mol)	E_{gap} (eV)	L (Å)	d (Å)	E_{str} (kJ/mol)	E_{gap} (eV)
(24 0)	3.87	32.8	21.9	4.2	3.76	31.0	8.1	4.5
(25 0)	3.87	34.0	20.7	4.2	3.77	32.0	7.5	4.4
(32 0)	3.85	42.5	14.8	4.1	3.79	40.3	4.4	4.1
(35 0)	3.85	46.1	13.1	4.1	3.80	43.6	3.7	3.9
(36 0)	3.85	47.3	12.6	4.1	3.80	44.8	2.9	3.9
(12 12)	5.45	24.5	19.8	4.3	5.40	22.1	27.3	4.3
(18 18)	5.43	34.7	13.6	4.2	5.37	32.0	6.3	3.7
(20 20)	5.43	38.1	12.3	4.1	5.38	35.4	3.9	3.7
(24 24)	5.43	45.0	10.0	4.1	5.38	42.2	1.0	3.7

[a] L Period, d maximal diameter, E_{str} strain energy, E_{gap} band gap (in slab: $a = 3.82$ Å; $E_{gap} = 3.9$ eV)

Table 7.2 Properties[a] of $SrTiO_3$ four-layer single-wall nanotubes

	Type I (SrO outer shell)				Type II (TiO_2 outer shell)			
Chirality	L (Å)	d (Å)	E_{str} (kJ/mol)	E_{gap} (eV)	L (Å)	d (Å)	E_{str} (kJ/mol)	E_{gap} (eV)
(28 0)	3.89	41.6	49.5	3.8	3.72	43.4	11.1	4.5
(30 0)	3.89	43.3	45.3	3.4	3.72	45.7	10.5	4.3
(32 0)	3.89	45.4	41.2	3.1	3.73	48.1	9.5	4.2
(48 0)	3.90	63.9	21.5	2.7	3.76	67.0	7.6	3.5
(12 12)	5.48	30.7	126.7	3.7	5.55	28.7	111.4	4.3
(15 15)	5.36	32.4	99.7	3.0	5.53	33.5	83.8	4.1
(16 16)	5.52	34.5	91.2	3.2	5.52	35.1	80.9	4.0
(24 24)	5.49	49.8	48.1	2.7	5.48	48.3	43.4	3.6

[a]L Period, d maximal diameter, w thickness, E_{str} strain energy, E_{gap} band gap (in slab: $a = 3.85$ Å; $E_{gap} = 2.6$ eV)

As a result, for any chirality and tube wall thickness w, there exists the minimum diameter below which NT is very unstable and undergoes spontaneous destruction. This also means that the ratio w/d should have an upper limit for each SWNT type rolled up from a single slab.

During the atomic relaxation, the period L of type I NTs is almost unchanged, while the period of type II NTs is slightly reduced relative to the initial (slab) value, except 4-layer NTs (n, n) where it is close for both types. The NT thickness w of 2-layer NTs is approximately the same as in a slab, while in 4-layer NTs w it varies from 5.5 to 6.5 Å due to the surface reconstruction observed in this case (see below).

The considered two-layer NTs exhibit a noticeable relaxation without the reconstruction of TiO_2 shell. In spite of the rolling effect, the length of Ti–O bond can be adjusted by the expansion or reduction of SrO shell, the covalent component of chemical bonds in which it is weak. More interesting results should be expected for 4-layer NTs because they provide more realistic models of NTs observed experimentally. Computer facilities allow us to calculate 4-layer NTs with chiralities up to (48, 0) and (24, 24) which comprise 480 atoms. Relatively stable 4-layer NTs arise at greater diameters than 2-layer NTs because of the large curvature difference between the inner and outer shells provoking considerable stretching and shrinking of the external and internal NT surfaces.

The initial diameter of type I 4-layer NTs (n, 0) is slightly reduced and its inner surface exhibits corrugation (see Fig. 7.2a). At the same time, the diameter of type II NT (n, 0) increases and the external NT surface undergoes a very prominent reconstruction which is accompanied by the breaking of some transverse (equatorial) Ti–O bonds and producing short (1.75 Å) Ti = O (titanyl) bonds (see Fig. 7.2b). Accordingly, the reflection planes passing through the tube axis disappear and the symmetry is reduced to C_{nh}.

In (n, n) case we observe the increase of 4-layer NT diameter during the atomic relaxation of both surface types. For type II NT (Fig. 7.2d) we again find a considerable reconstruction of the external surface layer. Its optimized structure is composed of isolated TiO_2 fragments (which, however, are connected to the

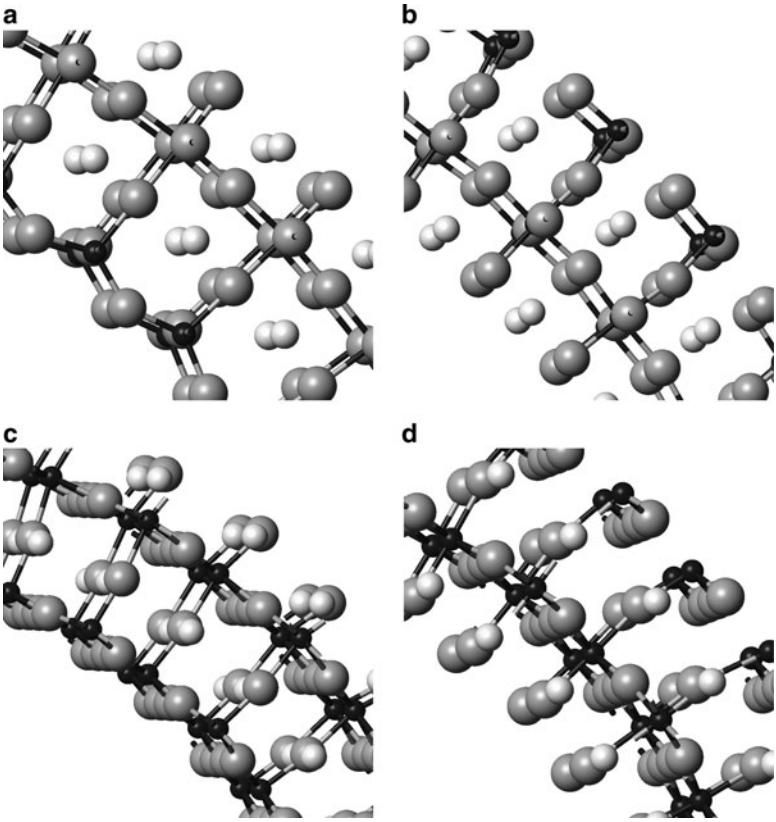

Fig. 7.2 Structure of $SrTiO_3$ SWNTs consisting of four atomic layers with different chirality (view along the tube axis). Chirality (48, 0): (**a**) type I with SrO outer shell; (**b**) type II with TiO_2 outer shell. Chirality (24, 24): (**c**) type I with SrO outer shell; (**d**) type II with TiO_2 outer shell. See Fig. 7.1 for legend

underneath oxygen atoms by normal Ti–O bond with the length of 1.81 Å). The lengths of two Ti=O bonds in TiO_2 fragment are equal to 1.77 Å. The NT symmetry is reduced to C_{2nh}.

In accordance with our expectations, the strain energy falls down upon the increasing the width of the NTs (see Tables 7.1 and 7.2). Nanotubes (n, 0) with TiO_2 external surface appear to be the most stable, and their stability depends on the tube diameter to a small extent. It is interesting, that the break of Ti–O bonds on the tube external surface does not influence this stability. Those tubes also have a high value of the band gap which is greater than the corresponding bulk (3.8 eV) and slab values (see Tables 7.1 and 7.2). The band gap is indirect at (n, 0) chirality, and direct at (n, n) chirality for both 2- and 4-layer NTs. The low strain energy is also attributed to 2-layer NTs (n, n) with TiO_2 external surface at $n > 16$.

7.4 Construction and Reformation of Double-Wall Nanotubes

We construct DWNT initial structures by combining two 2-layer SWNTs of the same type with different diameters so that the initial intertube distance $\Delta w_{12}{}^0$ (the difference between the inner radius of a larger one and the outer radius of a smaller one) is 3–5 Å. The adopted DWNTs are composed of about 300 atoms altogether. We have attempted to use chiralities with n_1 and n_2 having the large greatest common divisor N to preserve the rotational symmetry as much as possible. Finally, we have studied 6 SWNTs at (n_1, 0)@(n_2, 0) chirality and 4 SWNTs at (n_1, n_1)@(n_2, n_2) chirality with equal representation of types I and II (Table 7.3).

Two-layer single-wall NTs chosen as components for DWNTs do not exhibit the surface reconstruction described above for 4-layer SWNTs when they are optimized separately. However, the most important result obtained via optimization of DWNTs composed of 2-layer SWNTs is that the final structures of DWNTs differ from the initial structures drastically if $\Delta w_{12}{}^0 \leq 4.5$–$5.0$ Å depending on the SWNT type. The single-wall components exhibit almost the same structure as their isolated states do when the intertube distance is about 5 Å. Thus, in Fig. 7.3a, b we show the optimized structures of two NT types at chirality (24 0)@(36 0). Both walls preserve a cylindrical shape with symmetry properties considered in Sect. 7.2. The similar behavior has been found for type II DWNT at chirality (12 12)@(20 20) with the initial intertube distance of 4.7 Å (Fig. 7.4b). As it can be seen from Table 7.3, the binding energy for those tubes is very close to 0. This confirms a very weak interaction between the constituents. On the other hand, they have a large positive reformative energy, which presupposes their instability relative to 4-layer SWNTs with the same total number of atoms. The energy band gap of such DWNTs is very small (1.2–1.4 eV).

Table 7.3 Properties[a] of $SrTiO_3$ four-layer double-wall nanotubes

Chirality	L (Å)	$\Delta w_{12}{}^0$ (Å)	d (Å)	E_{bind} (kJ/mol)	E_{ref} (kJ/mol)	E_{gap} (eV)
		Type I (SrO outer shell)				
(24 0)@(32 0)	3.83	2.91	41.4	−97.3	−28.0	3.39
(25 0)@(35 0)	3.79	4.11	45.5	−84.9	−13.0	3.50
(24 0)@(36 0)	3.86	5.33	47.2	−0.1	71.8	1.44
(12 12)@(18 18)	5.42	3.20	33.8	−105.3	−88.4	2.92
(12 12)@(20 20)	5.40	4.91	34.9	−89.2	−64.8	3.20
		Type II (TiO_2 outer shell)				
(24 0)@(32 0)	3.79	2.58	41.6	−72.5	21.2	3.40
(25 0)@(35 0)	3.78	3.77	44.3	−65.1	28.4	3.34
(24 0)@(36 0)	3.79	4.85	44.7	−0.2	93.3	1.32
(12 12)@(18 18)	5.43	2.96	32.8	−46.2	−15.8	2.83
(12 12)@(20 20)	5.38	4.66	35.4	0.0	31.3	1.20

[a]L Period, $\Delta w_{12}{}^0$ initial intertube distance (using relaxed SWNT internal and external diameters), d maximal diameter, E_{bind} binding energy, E_{ref} reformative energy, E_{gap} band gap

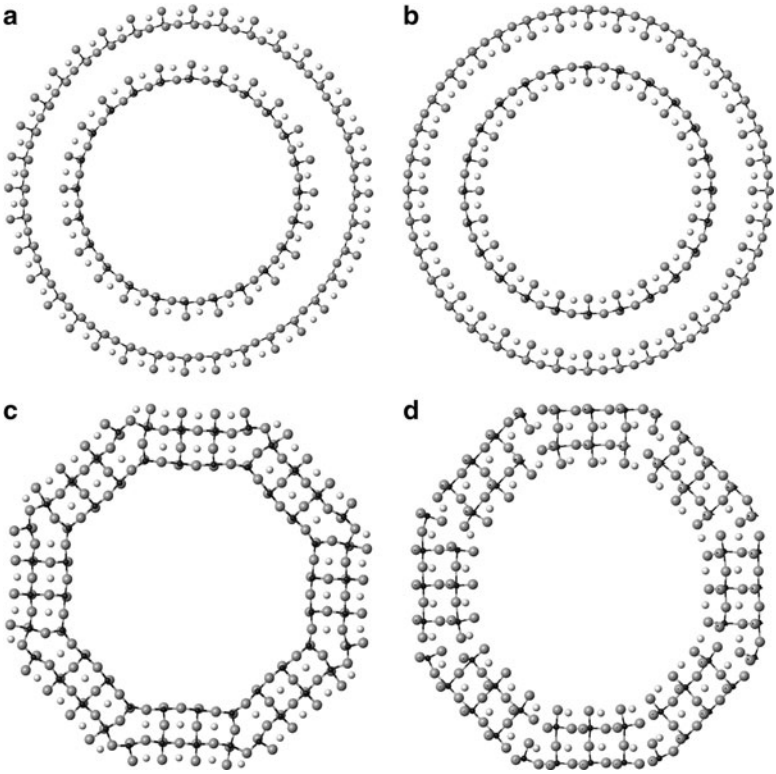

Fig. 7.3 Cross-view of $SrTiO_3$ (reformed) DWNTs with (n_1, 0)@(n_2, 0) chirality and SrO (**a**, **c**) and TiO_2 (**b**, **d**) outer terminations: (**a**, **b**) (24, 0)@(36, 0); (**c**, **d**) (24, 0)@(32, 0). See Fig. 7.1 for legend

In all other considered DWNTs two original SWNTs merge with a single-wall object upon the geometry optimization (see Figs. 7.3c, d and 7.4a, c, d). In these cases, the initial interwall distances are less than 5.0 Å for the SrO-terminated tubes and less than 4.5 Å for TiO_2-terminated tubes. For example, in initially double-wall nanotubes (24 0)@(32 0) $\Delta w_{12}{}^0$ is about 3 Å. The obtained NT-like objects resemble a polygon in cross-section and consist of 4-layer blocks with a distorted cubic perovskite structure. The number of blocks is equal to the order of rotation axis which is the common divisor N of the initial SWNT chiralities. The blocks are connected to each other by strongly reconstructed zones with partially broken Ti–O bonds. It should be noted, that this final shape does not depend on the explicit use of the rotational symmetry – we have obtained the same results in several test runs with the relaxed rotational symmetry constraints. All the obtained polyhedron-shaped NTs are remarkably stable relative to the 2-layer SWNT components; their binding energy varies from −50 to −100 kJ/mol. The NTs with SrO-terminated outer surface are also stable relative to reformation in the 4-layer SWNT (see E_{ref} in Table 7.3). The same is also true for NTs with initial chirality

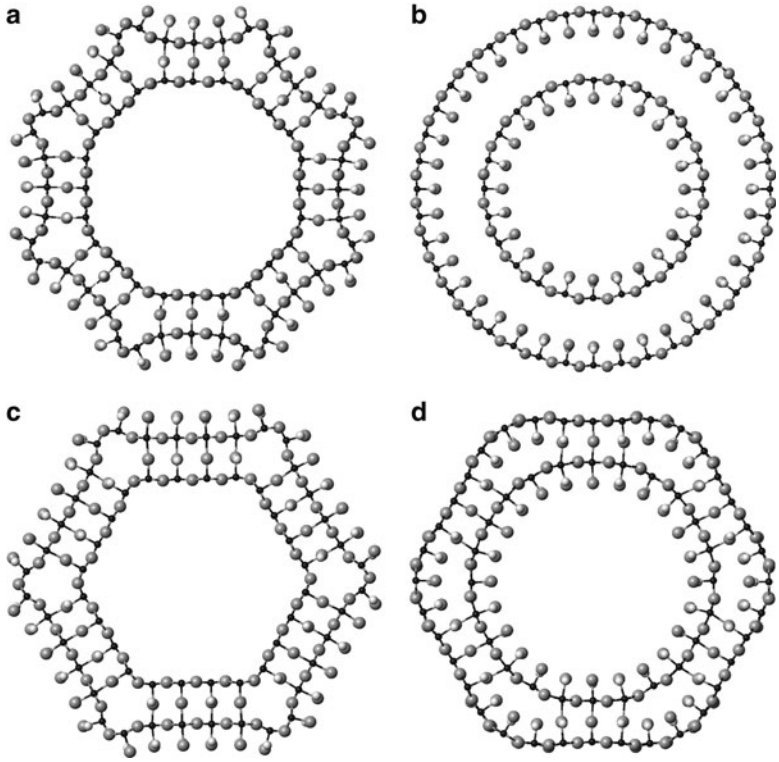

Fig. 7.4 Cross-view of $SrTiO_3$ (reformed) DWNTs with $(n_1, n_1)@(n_2, n_2)$ chirality and SrO (**a**, **c**) and TiO_2 (**b**, **d**) outer terminations: (**a**, **b**) (12, 12)@(20, 20); (**c**, **d**) (12, 12)@(18, 18). See Fig. 7.1 for legend

(12 12)@(18 18) and TiO_2-terminated outer surface, but the stability of type I tubes is greater. The energy band gap of polyhedron-shaped NTs is less than that of 2-layer components, but it is larger than the band gap of 4-layer slab (2.6 eV) and close to that of 4-layer NTs.

The observed [2] STO NTs have rather thick walls, $w > 20$ Å, with the ratio w/d of about 0.25. Obviously, tubes of this type cannot be rolled up from a single STO slab with such thickness. As it can be proved, the difference between the outer and inner circumferences of such a tube will be so big that interatomic distances on the outer shell will be two times longer than those on the inner shell, which is impossible. By this reason, the STO NTs with a large w/d ratio should either be multiwall or be composed of nanoblocks. The last case is really observed in Ref. [3] where it has been experimentally found that the tube walls are constructed of polycrystalline STO, which occasionally appears in the form of cube-like nanocrystals of various sizes. We can suppose that polyhedron-shaped NTs obtained in this study can be used as the simplest model for the real STO tubes with thick walls.

7.5 Conclusions

The considered two-layer single-wall $SrTiO_3$ nanotubes exhibit a noticeable relaxation without reconstruction of both shells. However, the inner or outer TiO_2 shells of four-layer single-wall nanotubes undergo a considerable reconstruction due to shrinkage or stretching of interatomic distances in the initial cubic perovskite structure.

There has been found two types of single-wall nanotube reconstruction: (1) breaking of Ti–O bonds with creation of Ti=O titanyl groups in the outer surface; (2) the inner surface folding due to Ti–O–Ti bending.

Two- and four-layer single-wall nanotubes at chirality (n, 0) with TiO_2 outer shell exhibit a relatively big stability and a large value of the band gap.

Double-wall $SrTiO_3$ nanotubes constructed from two-layer nanotubes show different stability depending on the initial intertube distance. At the intertube distance greater than 5 Å, single-wall components exhibit a weak interaction. At smaller intertube distances, two single-wall components merge to form polyhedron-shaped tubular objects. Those NT-like objects have a polygon in the cross-section and consist of 4-layer blocks with a distorted cubic perovskite structure.

In contrast to single-wall nanotubes, the four-layer tubular objects with a SrO-terminated surface demonstrate the maximum stability. High stability of such structures allows considering them as reliable models of perovskite nanotubes.

Acknowledgements The authors are grateful for the support to Saint Petersburg State University (grant 12.37.142.2011) and to RBRF (grant 11-03-00466a).

References

1. Hernandez BA, Chang K-S, Fisher ER, Dorhout PK (2002) Sol-gel template synthesis and characterization of $BaTiO_3$ and $PbTiO_3$ nanotubes. Chem Mater 14(2):480–482
2. Mao Y, Banerjee S, Wong SS (2003) Hydrothermal synthesis of perovskite nanotubes. Chem Commun 3:408–409
3. Žagar K, Rečnik A, Ajayan PM, Čeh M (2010) Oriented cube-on-cube nanocrystal assembly of $SrTiO_3$ tubules. Nanotechnology 21:375605 (1–7)
4. Bandura A, Evarestov R, Oranskaya A (2011) LCAO calculations of $SrTiO_3$ nanotubes. In: Book of abstracts of international conference "Functional Materials and Nanotechnologies-2011", University of Latvia, Riga, p 66
5. Damnjanović M, Nikolić B, Milošević I (2007) Symmetry of nanotubes rolled up from arbitrary two-dimensional lattices along an arbitrary chiral vector. Phys Rev B 75:033403 (1–4)
6. Damnjanović M, Milošević I, Vuković T, Sredanović R (1999) Full symmetry, optical activity, and potentials of single-wall and multiwall nanotubes. Phys Rev B 60(4):2728–2739
7. Evarestov R (2011) Symmetry and structure of $SrTiO_3$ nanotubes. In: Book of abstracts of international conference "Functional Materials and Nanotechnologies-2011", University of Latvia, Riga, p 28

8. Dovesi R, Saunders VR, Roetti C, Orlando R, Zicovich-Wilson CM, Pascale F, Civalleri B, Doll K, Harrison NM, Bush IJ, D'Arco P, Llunell M (2010) CRYSTAL09 user's manual. University of Torino, Torino
9. LaJohn LA, Christiansen PA, Ross RB, Atashroo T, Ermler WC (1987) Ab initio relativistic effective potentials with spin-orbit operators. III. Rb through Xe. J Chem Phys 87 (5):2812–2824
10. Evarestov RA, Zhukovskii YuF, Bandura AV, Piskunov S (2011) Symmetry and models of single-walled TiO_2 nanotubes with rectangular morphology. Cent Eur J Phys 9(2):492–501
11. Padilla J, Vanderbilt D (1998) Ab initio study of $SrTiO_3$ surfaces. Surf Sci 418:64–70
12. Heifets E, Eglitis RI, Kotomin EA, Maier J, Borstel G (2001) Ab initio modeling of surface structure for $SrTiO_3$ perovskite crystals. Phys Rev B 64:235417 (1–5)